

2. CALCAREOUS NANNOFOSSIL BIOSTRATIGRAPHY OF THE EOCENE– OLIGOCENE TRANSITION, ODP SITES 1123 AND 1124¹

Kristeen McGonigal² and Agata Di Stefano³

ABSTRACT

Seven sites were drilled off the eastern shore of New Zealand during Ocean Drilling Program Leg 181 to gain knowledge of southwest Pacific ocean history, in particular, the evolution of the Pacific Deep Western Boundary Current (DWBC). Holes 1123C and 1124C penetrated lower Oligocene to middle Eocene sediments containing moderately to poorly preserved calcareous nannofossils. Nannofossil assemblages show signs of dissolution and overgrowth, but key marker species can be identified. Nannofossil abundance ranges from abundant to barren. The lower Oligocene sediments are distinctly separated from the overlying Neogene sequences by the Marshall Paraconformity, a regional marker of environmental and sea level change. An age-depth model for Hole 1123C through this sequence was constructed using nine nannofossil age datums and three magnetostratigraphic datums. There is good agreement between the biostratigraphy and magnetostratigraphy, which indicates that the Marshall Paraconformity spans ~12 m.y. in Hole 1123C. The same sequence in Hole 1124C is disrupted by at least three hiatuses, complicating interpretation of the sedimentation history. The Marshall Paraconformity spans at least 3 m.y. in Hole 1124C. A 4- m.y. gap separates lower Oligocene and middle Eocene sediments, and a ~15 m.y. hiatus separates middle Eocene mudstones from middle Paleocene nannofossil-bearing mudstones. Nannofossil biostratigraphy from Holes 1123C and 1124C indicates that the Eocene–Oligocene

¹McGonigal, K., and Di Stefano, A., 2002. Calcareous nannofossil biostratigraphy of the Eocene–Oligocene transition, ODP Sites 1123 and 1124. *In* Richter, C. (Ed.), *Proc. ODP, Sci. Results*, 181, 1–22 [Online]. Available from World Wide Web: <http://www-odp.tamu.edu/publications/181_SR/VOLUME/CHAPTERS/207.PDF>. [Cited YYYY-MM-DD]

²Department of Geological Sciences, 108 Carraway Building, Florida State University, Tallahassee FL 32306, USA. roessig@gly.fsu.edu

³Dipartimento di Scienze Geologiche, Università di Catania, Corso Italia 55, 95129 Catania, Italy.

transition was a time of fluctuating biota and intensification of the DWBC along the New Zealand margin.

INTRODUCTION

The Eocene–Oligocene transition marks the change in Earth’s climate from a “greenhouse” climate to an “icehouse” climate, a theory first postulated by Kennett, Houtz, et al. (1975). This climatic deterioration has been linked to the beginning of circumpolar current flow and the thermal isolation of Antarctica. New Zealand is a prime area to look for evidence of paleoceanographic changes across this transition as it is located downcurrent from the Tasman Seaway, a primary gateway for the evolving Antarctic Circumpolar Current.

Ocean Drilling Program (ODP) Holes 1123C and 1124C penetrated the Eocene–Oligocene transition sequences east of New Zealand (Fig. F1). Site 1123 is located on the Campbell Plateau, 410 km northeast of the Chatham Islands (Shipboard Scientific Party, 1999a). The extended core barrel (XCB) system was used to recover the Oligocene and Eocene sediments. These sediments consist of alternating white clay-bearing nannofossil chalk and light greenish gray clayey nannofossil chalk overlying alternating white and light gray micritic limestone. Clay residues and stylolitic surfaces beginning in Core 181-1123C-30X indicate advanced diagenesis and pressure dissolution (Shipboard Scientific Party, 1999b), which coincides with increasingly poor nannofossil preservation (Table T1).

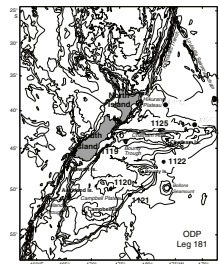
Site 1124 is located ~600 km due east of the North Island on the Rekohu Drift (Fig. F1), a turbidite overbank deposit southeast of the Hikurangi Channel (Shipboard Scientific Party, 1999a). Oligocene and Eocene sediments were recovered with the XCB and consist of sharply contrasting lithologies including light greenish gray to white nannofossil chalk, red, yellow, pink, and brown mudstone, and nannofossil-bearing mudstone (Shipboard Scientific Party, 1999c). Three distinct disconformities separate these lithologies, and poor nannofossil preservation in the mudstones complicates interpretation of this 20 m sequence.

This study reports the nannofossil biostratigraphy through the Eocene–Oligocene sequences recovered in ODP Holes 1123C and 1124C. Nannofossil datums are used in conjunction with magnetostratigraphic datums to calculate linear sedimentation rates (LSRs) for these sequences.

PREVIOUS WORK

Leg 181 was the first ODP leg to drill the New Zealand margin. The margin had previously been drilled during two Deep Sea Drilling Project (DSDP) legs. During DSDP Leg 29, 10 sites around New Zealand and Australia were drilled. Sites 275, 276, and 277 were drilled on the southern edge of the Campbell Plateau. Oligocene and Eocene nannofossils were observed at Sites 276 and 277 (Edwards and Perch-Nielsen, 1975). At Site 277, a continuous upper Oligocene through Eocene sequence was recovered. Site 277 was reanalyzed to produce an integrated biostratigraphy (Hollis et al., 1997) between foraminifers, calcareous nannofossils, radiolarians, and palynomorphs. This analysis suggests

F1. Bathymetric map, eastern New Zealand region, showing Leg 181 drillsites, p. 11.



T1. Stratigraphic distribution of calcareous nannofossils, Hole 1123C, p. 16.

that environmental deterioration in the southwest Pacific was episodic and began in the late Eocene to earliest Oligocene.

Eocene–Oligocene sections were recovered during DSDP Leg 90 at Sites 588C, 592, and 593, all located between Australia and New Zealand. Nannofossil biostratigraphy indicates a ~20-m.y. hiatus at Site 588C encompassing late Eocene–early Oligocene Zones NP17–NP23. Early Oligocene to early Miocene Zones NP22–NN2 encompassing ~16 m.y. are missing at Site 592. This early Oligocene to early Miocene hiatus is similar to that at Site 1123C. Biostratigraphic placement of the Eocene/Oligocene boundary could not be achieved at Site 593 because of volcanogenic input. No hiatus in the Oligocene to early Miocene was reported (Martini, 1986).

METHODS

Standard nannofossil smear slide techniques were used to prepare samples. Unprocessed sediment was smeared on a glass coverslip, dried, and then mounted on a glass slide using Norland optical adhesive 61 mounting media. The nannofossil biostratigraphy presented here is based on the examination of each sample using a Zeiss Photomicroscope III under 625× – 1560× magnification, using phase-contrast, plain, and cross-polarized light. Several traverses were made, and relative abundance of individual species, overall abundance of nannofossils, and assemblage preservation were recorded for each sample using BugWin software (BugWare, Inc.).

Range charts presented herein as Tables **T1** and **T2** were created using these measurements. Individual species abundance are represented by the following abbreviations:

- V = very abundant (more than 100 specimens per 10 fields of view [FOV]).
- A = abundant (11–100 specimens per 10 FOV).
- C = common (6–10 specimen per 10 FOV).
- F = few (1–5 specimen per 10 FOV).
- R = rare (1 specimen per >10 FOV).

The same definitions were used for estimations of total abundance of nannofossils within each sample, with the additional definition of B (barren of nannofossils). Preservation of the calcareous nannofossil assemblage was determined as follows:

- G = good (individual specimens exhibit little or no dissolution or overgrowth, diagnostic characteristics are preserved, and nearly all of the specimens can be identified).
- M = moderate (individual specimens show evidence of dissolution or overgrowth, some specimens cannot be identified to the species level).
- P = poor (individual specimens exhibit considerable dissolution or overgrowth, many specimens cannot be identified to the species level).

Calcareous nannofossil species considered in this paper are listed in “**Appendix**,” p. 10, where they are arranged alphabetically by generic epithet. Bibliographic references for these taxa can be found in Perch-

T2. Stratigraphic distribution of calcareous nannofossils, Hole 1124C, p. 18.

Nielsen (1985) and Bown (1998). Key marker species were photographed (Plate P1).

ZONATION

The standard zonal schemes of Martini (1971) and Okada and Bukry (1980) are used for Leg 181 Eocene and Oligocene sediments (Fig. F2). Middle Eocene (NP16/CP14a) through late Oligocene (NP25/CP19b) zones are represented with Zones NP17/CP14b, NP18/CP15a, NP23/CP17–18, and NP24/CP19a missing because of multiple hiatuses. Zones NP19 and NP20 (Martini, 1971) were combined because *Sphenolithus pseudoradians* was rarely present in only a few samples from Hole 1124C. The high-latitude zonal scheme of Wei and Wise (1990) was not used since *Reticulofenestra oamaruensis* was not identified because of poor preservation.

In the Martini (1971) and Okada and Bukry (1980) nannofossil zonal schemes, the Eocene/Oligocene boundary is approximated by the last occurrence (LO) of the large-bodied discoasters *Discoaster barbadiensis* (34.3 Ma) and *Discoaster saipanensis* (34.2 Ma). This classical nannofossil event is older than the global stratotype section and point (GSSP) recognized Eocene/Oligocene boundary (Coccioni et al., 1988; Premoli Silva and Jenkins, 1993) based on the extinction of the foraminiferal genus *Hantkenina* (33.7 Ma).

BIOSTRATIGRAPHIC RESULTS

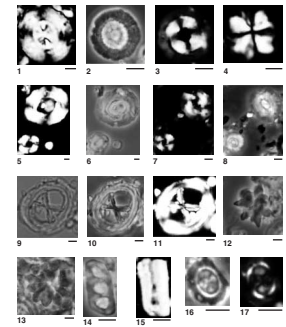
Hole 1123C Summary

Coring of Hole 1123C (41°47.147'S, 171°29.941'W; water depth = 3290.1 m) began with the advanced hydraulic piston core system and was washed down from 151.5 meters below seafloor (mbsf) to 484.0 mbsf, with one XCB core taken at 230.0 mbsf. Early Miocene sediments in Sample 181-1123C-29X-2, 97–98 cm, have an age of ~ 21.7 Ma based on linear sedimentation rate (LSR) extrapolation (Shipboard Scientific Party, 1999b). Immediately below this bioturbated boundary (Fig. F3), continuous upper Eocene–lower Oligocene sediments were recovered between Samples 181-1123C-29X-2, 110–111 cm, and 33X-CC, 14–15 cm. The Marshall Paraconformity that separates the lower Miocene sediments from the lower Oligocene sediments spans ~12 m.y., based on calcareous nannofossil and magnetostratigraphic datums (Fig. F4).

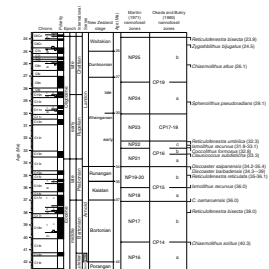
Stratigraphic distribution of nannofossils from Hole 1123C is recorded in Table T1. Key biohorizons are listed in Table T3, along with their sample interval and average depth. These sediments consist mainly of alternating white clay-bearing nannofossil chalk with light greenish gray clayey nannofossil chalk and alternating white and light gray micritic limestone. Calcareous nannofossils are abundant in most samples, and their preservation is moderate to poor, declining downsection.

The *Reticulofenestra hillae* Subzone (NP22/CP16c) ranges from Samples 181-1123C-29X-2, 110–111 cm, to 29X-4, 61–62 cm, based on the presence of *Reticulofenestra umbilica* and the absence of *Coccolithus formosus*. Reworked *C. formosus* are rare through this interval but are easily identified because of more intensive overgrowth compared to the rest of the assemblage. *Chiasmolithus altus*, *Coccolithus pelagicus*, *Ismolithus*

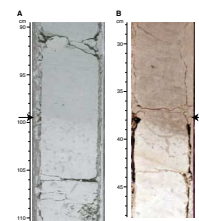
P1. Light micrographs, p. 22.



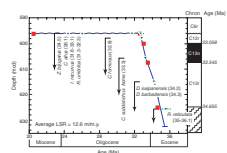
F2. Eocene and Oligocene calcareous nannofossil biostratigraphic datum, New Zealand stages, and zonal units, p. 12.



F3. Marshall Paraconformity for two intervals, p. 13.



F4. Age-depth plot, Hole 1123C, p. 14.



T3. Calcareous nannofossil and magnetostratigraphic events, Hole 1123C, p. 20.

recurvus, *Reticulofenestra bisecta*, *R. umbilica*, and *Reticulofenestra samodurovii* are common components of the assemblage. Nannofossils are very abundant to common and moderately to poorly preserved.

Samples 181-1123C-29X-4, 110–111 cm, through 30X-2, 66–67 cm, represent the *Coccolithus formosus* Subzone (NP21/CP16b), marked by the presence of *C. formosus*. Nannofossils are abundant and moderately to poorly preserved in this assemblage, characterized by *C. altus*, *C. pelagicus*, *I. recurvus*, *R. bisecta*, and *R. umbilica*.

The acme of *Clausicoccus subdistichus* denotes that Sample 181-1123C-30X-2, 114–115 cm, belongs to the *Coccolithus subdistichus* Subzone (NP21/CP16a). This assemblage is represented by moderately preserved and abundant *C. subdistichus*, *C. formosus*, *C. pelagicus*, *I. recurvus*, *R. bisecta*, *R. umbilica*, and *R. samodurovii*.

The Eocene/Oligocene boundary, based on calcareous nannofossils, is placed between Samples 181-1123C-31X-2, 10–11 cm, and 31X-2, 60–61 cm, denoted by the LO of *Discoaster saipanensis* (34.2 Ma) and *D. bardiensis* (34.3 Ma). This boundary is ~0.5 m.y. older than the boundary based on the LO of *Hantkenina* spp. (33.7 Ma). The GSSP Eocene/Oligocene boundary is estimated at 610.7 meters composite depth (mcd), based on LSR extrapolation.

Samples 181-1123C-31X-2, 60–61 cm, to 33X-CC, 14–15 cm (bottom of Hole 1123C) represent the late Eocene *Ismolithus recurvus* Subzone (CP15b) of Okada and Bukry (1980) or the combined NP19/NP20 Zones of Martini (1971). The absence of *Sphenolithus pseudoradians* precludes the separation of Martini Zones NP19 and NP20. Nannofossils are very abundant to abundant and moderately to poorly preserved. The nannofossil assemblage is represented by *Bicolumnus ovatus*, *Chiasmolithus omaurensis*, *Coccolithus formosus*, *C. pelagicus*, *D. deflandrei*, *Ismolithus recurvus*, *Reticulofenestra bisecta*, *R. umbilica*, and *R. samodurovii*. Based on the presence of *Ismolithus recurvus* (first occurrence 36 Ma) and extrapolation of linear sedimentation rates (Fig. F4), the bottom of Hole 1123C is estimated at 35.8 Ma

Hole 1124C Summary

Coring of Hole 1124C (39°29.901'S, 176°31.894'W; water depth = 3966.5 m) began at 8.0 mbsf (Fig. F1) and recovered Pleistocene through Late Cretaceous sediments. Middle Eocene–early Oligocene sediments were recognized between Samples 181-1124C-43X-1, 10–11 cm, and 44X-CC, 13–14 cm, with major unconformities between upper and lower Oligocene, in the lowest Oligocene, between lower Oligocene and middle Eocene, and between middle Eocene and middle Paleocene sections. Calcareous nannofossils are abundant through the majority of this section with abundance declining in the increasingly brown mudstones. Preservation is moderate in the white to light greenish gray nannofossil chalk, degrading to poor in the yellow-brown and red-brown nannofossil-bearing silty mudstone, becoming barren in the dark grayish brown mudstone. Ranges of calcareous nannofossils considered in this study and their abundance and preservation are listed in Table T2, and key biohorizons, sample intervals, and average depths are listed in Table T4.

The *Sphenolithus predistensus* Zone (NP25/CP19b) ranges from Samples 181-1124C-43X-1, 10–11 cm, to 43X-2, 10–11 cm, based on the presence of *Reticulofenestra bisecta* and *Chiasmolithus altus*. Reworked specimens of *R. umbilica* and *Coccolithus formosus* are also present. Between Samples 181-1124C-43X-2, 10–11 cm, and 43X-3, 60–61 cm, a

T4. Calcareous nannofossil and magnetostratigraphic events, Hole 1124C, p. 21.

hiatus of 3–5 m.y. is present (Shipboard Scientific Party, 1999c). The bioturbated interval at Section 181-1124C-43X-2, 38 cm, is interpreted to represent the Marshall Paraconformity (Fig. F3), separating upper and lower Oligocene sediments. Chiasmoliths, *Cyclocargolithus floridanus*, and reticulofenestrids dominate the moderately preserved nannofossil assemblage.

Below the Marshall Paraconformity is the lower Oligocene *Clausicoccus subdistichus* Zone (NP21/CP16a–b). Samples 181-1124C-43X-6, 60–61 cm, through 43X-6, 110–111 cm, are included in this zone. Nannofossils are abundant and moderately well preserved in the white nannofossil chalk. The assemblage is characterized by *Bicolumnus ovatus*, *Blackites spinosus*, *Chiasmolithus altus*, *Clausicoccus subdistichus*, *Coccolithus formosus*, *Ismolithus recurvus*, *Reticulofenestra bisecta*, *R. umbilica*, and *R. samodurovii*. A sharp contact was noted between Sample 181-1124C-44X-1, 3–4 cm, composed of greenish nannofossil chalk, and the reddish mudstone of Core 181-1124C-44X. Nannofossils from the chalk indicate that it is early Oligocene in age and is considered to be a piece of fall-in from farther uphole.

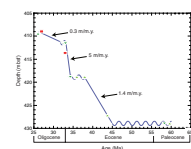
Samples 181-1124C-44X-1, 10–11 cm, through 44X-CC, 13–14 cm, represent the middle Eocene *Chiasmolithus solitus* Zone (NP16/CP14a), marked by the appearance of the large-bodied discoasters *Discoaster saipanensis* and *D. barbadiensis*. Based on LSRs, an ~4-m.y. hiatus separates these two cores. Nannofossils are abundant and poorly preserved in the red, yellow, and pink bioturbated mudstones. Preservation declines downsection as the sediments grade to brown mudstone, with Sample 181-1124C-44X-7, 10–11 cm, being barren of nannofossils. *Coccolithus formosus*, *C. pelagicus*, *D. barbadiensis*, *D. deflandrei*, *D. saipanensis*, *Reticulofenestra umbilica*, and *R. samodurovii* typify this assemblage.

Nannofossils are abundant again in Core 181-1124C-45X-1. The presence of *Fasiculithus tympaniformis* and *Hornibrookina teuriensis* in the nannofossil-bearing light brown mudstone indicates that the top of Core 181-1124C-45X is a middle Paleocene age of ~58 Ma (Shipboard Scientific Party, 1999c). This indicates a 15-m.y. hiatus between Cores 181-1124C-44X and 45X based on LSR extrapolation. The sediment from 181-1124C-45X-1, 0–5 cm, consists of greenish nannofossil chalk lying sharply on white nannofossil chalk. This sample is considered to be fall-in from farther uphole.

LINEAR SEDIMENTATION RATES

LSRs were calculated for each site and plotted with visual best-fit lines. The average sedimentation rate at Hole 1123C is 12.6 m/m.y. Nannofossil age dates are in good agreement with the magnetostratigraphic interpretation (Fig. F4). Sedimentation rates vary from 9 to 16.4 m/m.y. and are reasonable rates for biogenic ooze accumulation in open-ocean conditions with little terrigenous input. Sedimentation rates for Hole 1123C (Fig. F4) are based on nine nannofossil bioevents and four magnetostratigraphic events (Table T3). Hole 1124C LSRs range from 0.3 to 5 m/m.y. Hole 1124C LSRs (Fig. F5) are based on 11 nannofossil bioevents and two magnetostratigraphic events (Table T4), with four hiatuses within the 20-m interval. Nannofossil age estimates (Fig. F2) are taken from Berggren et al. (1995).

F5. Age-depth plot, Hole 1124C, p. 15.



CONCLUSION

Lower Oligocene through middle Eocene sediments recovered along the New Zealand margin during ODP Leg 181 contain abundant, moderately preserved calcareous nannofossils in chalks and limestones, whereas mudstones are impoverished to barren. Key calcareous nannofossil marker species in conjunction with magnetostratigraphic data were used to create age-depth plots for Holes 1123C and 1124C. Sedimentation rates ranged from 0.3 to 16 m/m.y. in the lower Oligocene to middle Eocene sequences. Sites 1123 and 1124 both reveal an early Oligocene hiatus, the Marshall Paraconformity (Carter and Landis, 1972; Carter, 1985; Fulthorpe et al., 1996). Although bioturbated, the disconformity is marked by a clear break in the nannofossil assemblage and by distinct changes in lithology (Fig. F3). It is interpreted to represent increased erosion by bottom waters associated with increased velocity of the DWBC in the early Oligocene. Holes 1123C and 1124C indicate that the Eocene–Oligocene transition along the New Zealand margin was a time of changing paleoceanographic conditions.

ACKNOWLEDGMENTS

We thank Drs. Wuchang Wei and James Pospichal for their critical review and helpful suggestions, which greatly improved this paper. We are grateful to Mitch Covington of BugWare for providing the counting software used in collecting the data. Samples were provided by the U.S. National Science Foundation (NSF) through the Ocean Drilling Program (ODP). This research used samples and/or data provided by ODP. ODP is sponsored by NSF and participating countries under management of Joint Oceanographic Institutions (JOI), Inc. A. Di Stefano was funded by MRST Cofin 1999 (9904152971) grants to Professor I. Premoli Silva. Laboratory facilities for K. McGonigal were provided by NSF grant No. DPP 94-22893.

REFERENCES

- Berggren, W.A., Kent, D.V., Swisher, C.C., III, and Aubry, M.-P., 1995. A revised Cenozoic geochronology and chronostratigraphy. In Berggren, W.A., Kent, D.V., Aubry, M.-P., and Hardenbol, J. (Eds.), *Geochronology, Time Scales and Global Stratigraphic Correlation*. Spec. Publ.—Soc. Econ. Paleontol. Mineral., 54:129–212.
- Bown, P.R. (Ed.), 1998. *Calcareous Nannofossil Biostratigraphy*: London (Chapman and Hall).
- Carter, R.M., 1985. The mid-Oligocene Marshall Paraconformity, New Zealand: coincidence with global eustatic sea-level fall or rise? *J. Geol.*, 93:359–371.
- Carter, R.M., and Landis, C.A., 1972. Correlative Oligocene unconformities in southern Australasia. *Nature*, 237:12–13.
- Coccioni, R., Monaco, P., Monechi, S., Nocchi, M., and Parisi, G., 1988. Biostratigraphy of the Eocene-Oligocene boundary at Massignano (Ancona, Italy). In Premoli Silva, I., Coccioni, R., and Montanari, A. (Eds.), *The Eocene-Oligocene Boundary in the Marche-Umbria Basin (Italy)*: Ancona (Int. Union Geol. Sci.), 59–80.
- Edwards, A.R., and Perch-Nielsen, K., 1975. Calcareous nannofossils from the southern southwest Pacific, DSDP Leg 29. In Kennett, J.P., Houtz, R.E., et al., *Init. Repts. DSDP, 29*: Washington (U.S. Govt. Printing Office), 469–539.
- Fulthorpe, C.S., Carter, R.M., Miller, K.G., and Wilson, J. 1996. The Marshall Paraconformity: a mid-Oligocene record of inception of the Antarctic circumpolar current and coeval glacio-eustatic lowstand. *Mar. Pet. Geol.*, 13:61–77.
- Hollis, C.J., Waghorn, D.B., Strong, C.P., and Crouch, E.M., 1997. *Integrated Paleogene Biostratigraphy of DSDP Site 277 (Leg 29): Foraminifera, Calcareous Nannofossils, Radiolaria, and Palynomorphs*: Lower Hutt (Inst. Geol. Nucl. Sci.).
- Kennett, J.P., Houtz, R.E., et al., 1975. *Init. Repts. DSDP, 29*: Washington (U.S. Govt. Printing Office).
- Martini, E., 1971. Standard Tertiary and Quaternary calcareous nannoplankton zonation. In Farinacci, A. (Ed.), *Proc. 2nd Int. Conf. Planktonic Microfossils Roma*: Rome (Ed. Tecnosci), 2:739–785.
- Martini, E., 1986. Paleogene calcareous nannoplankton from the southwest Pacific Ocean, Deep Sea Drilling Project, Leg 90. In Kennett, J.P., von der Borch, C.C., et al., *Init. Repts. DSDP, 90*: Washington (U.S. Govt. Printing Office), 747–761.
- Okada, H., and Bukry, D., 1980. Supplementary modification and introduction of code numbers to the low latitude coccolith biostratigraphic zonation (Bukry 1973, 1975). *Mar. Micropaleontol.*, 5:321–325.
- Perch-Nielsen, K., 1985. Cenozoic calcareous nannofossils. In Bolli, H.M., Saunders, J.B., and Perch-Nielsen, K. (Eds.), *Plankton Stratigraphy*: Cambridge (Cambridge Univ. Press), 427–554.
- Premoli Silva, I., and Jenkins, D.G., 1993. Decision on the Eocene/Oligocene boundary stratotype. *Episodes*, 16:379–382.
- Shipboard Scientific Party, 1999a. Leg 181 summary: Southwest Pacific paleoceanography. In Carter, R.M., McCave, I.N., Richter, C., Carter, L. et al., *Proc. ODP, Init. Repts.* [CD-ROM], 181: College Station, TX (Ocean Drilling Program), 1–80.
- , 1999b. Site 1123: North Chatham Drift—a 20-Ma record of the Pacific Deep Western Boundary Current. In Carter, R.M., McCave, I.N., Richter, C., Carter, L. et al., *Proc. ODP, Init. Repts.*, 181, 1–184 [CD-ROM]. Available from: Ocean Drilling Program, Texas A&M University, College Station, TX 77845-9547, U.S.A.
- , 1999c. Site 1124: Rekohu Drift—from the K/T boundary to the Deep Western Boundary Current. In Carter, R.M., McCave, I.N., Richter, C., Carter, L., et al., *Proc. ODP, Init. Repts.*, 181, 1–137 [CD-ROM]. Available from: Ocean Drilling Program, Texas A&M University, College Station, TX 77845-9547, U.S.A.
- Wei, W., and Wise, S.W., Jr., 1990. Middle Eocene to Pleistocene calcareous nannofossils recovered by Ocean Drilling Program Leg 113 in the Weddell Sea. In Barker, P.F.,

Kennett, J.P., et al., *Proc. ODP, Sci. Results*, 113: College Station, TX (Ocean Drilling Program), 639–666.

APPENDIX

Eocene and Oligocene Calcareous Nannofossil Species Considered in This Report

- Bicolumnus ovatus* Wei and Wise, 1992
Blackites spinosus (Deflandre and Fert, 1954) Hay and Towe (1962)
Chiasmolithus altus Bukry and Percival (1971)
Chiasmolithus expansus (Bramlette and Sullivan, 1961) Gartner (1970)
Chiasmolithus grandis (Bramlette and Sullivan, 1961) Radomski (1968)
Chiasmolithus oamaruensis (Deflandre, 1954) Hay, Mohler, and Wade (1966)
Chiasmolithus solitus (Bramlette and Sullivan, 1961) Locker (1968)
Clausicoccus subdistichus (Roth and Hay in Hay et al., 1967) Prins, 1979
Coccolithus eopelagicus (Bramlette and Riedel, 1954) Bramlette and Sullivan (1961)
Coccolithus formosus (Kamptner, 1963) Haq (1971)
Coccolithus pelagicus (Wallich, 1877) Schiller (1930)
Cyclicargolithus abisectus (Müller, 1970) Wise (1973)
Cyclicargolithus floridanus (Roth and Hay in Hay et al., 1967) Bukry (1971)
Cyclicargolithus lumina Sullivan (1965)
Discoaster adamanteus Bramlette and Wilcoxon (1967)
Discoaster barbadiensis Tan (1927)
Discoaster deflandrei Bramlette and Riedel (1954)
Discoaster saipanensis Bramlette and Riedel (1954)
Discoaster tanii Bramlette and Riedel (1954)
Discoaster tanii nodifer Bramlette and Riedel (1954)
Fasciculithus tympaniformis Hay and Mohler (1967)
Helicosphaera bramlettei Müller (1970)
Helicosphaera euphratis Haq (1966)
Hornibrookina teuriensis Edwards (1973)
Ismolithus recurvus (Deflandre in Deflandre and Fert, 1954) Bramlette and Martini (1964)
Markalius inversus (Deflandre in Deflandre and Fert, 1954) Bramlette and Martini (1964)
Nannotetrina fulgens (Stradner, 1960) Achuthan and Stradner (1969)
Reticulofenestra bisecta (Hay, Mohler, and Wade, 1966) Bukry and Percival (1971)
Reticulofenestra clatrata Müller (1970)
Reticulofenestra daviesii (Haq, 1968) Haq (1971)
Reticulofenestra perplexa (Burns 1975) Wise (1983)
Reticulofenestra reticulata (Gartner and Smith, 1967) Roth and Thierstein (1972)
Reticulofenestra samodurovii (Hay, Mohler, and Wade, 1966) Roth (1970)
Reticulofenestra umbilica (Levin, 1965) Martini and Ritzkowski (1968)
Rhabdosphaera scabrosa Deflandre in Deflandre and Fert (1954)
Rhabdosphaera tenuis Bramlette and Sullivan (1961)
Sphenolithus moriformis (Bronnimann and Stradner, 1960) Bramlette and Wilcoxon (1967)
Sphenolithus radians Deflandre in Grasse (1952)
Zygrhablithus bijugatus (Deflandre in Deflandre and Fert, 1954) Deflandre (1959)

Figure F1. Bathymetric map of the eastern New Zealand region, showing Leg 181 drill sites.

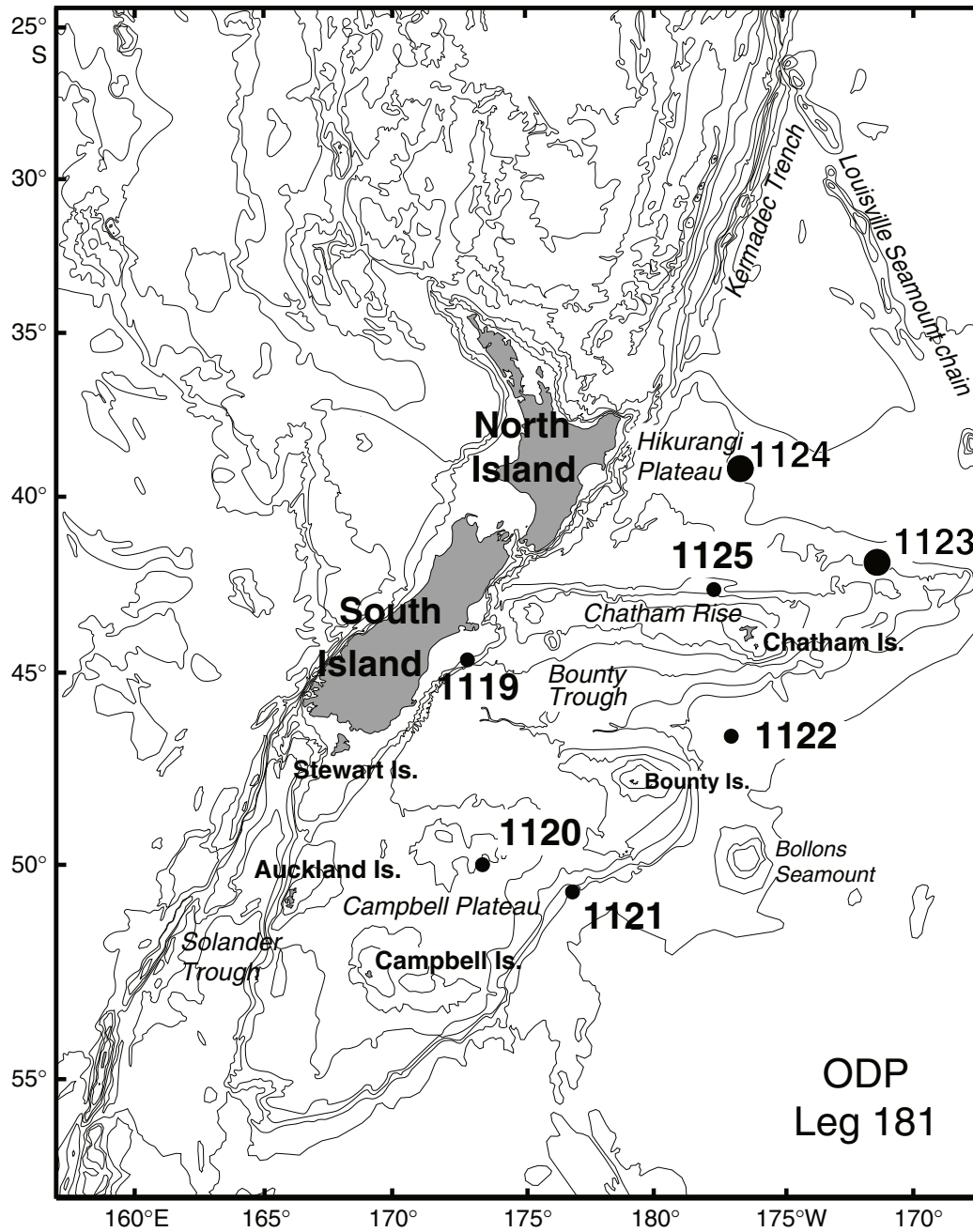


Figure F2. Eocene and Oligocene calcareous nannofossil biostratigraphic datums used in this report after Berggren et al. (1995). Also shown are New Zealand stages and the zonal units of Martini (1971) and Okada and Bukry (1980).

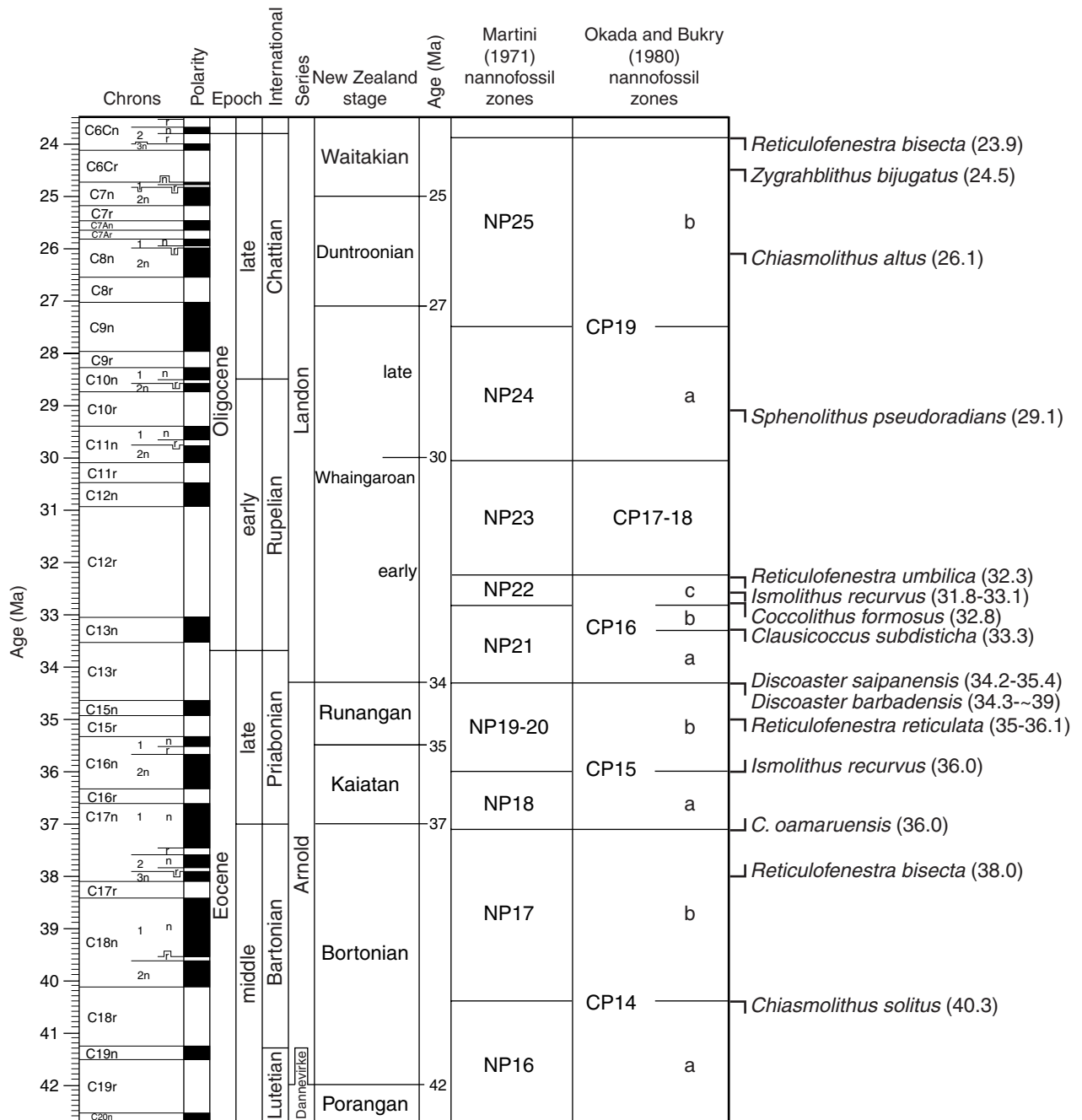


Figure F3. Marshall Paraconformity for (A) interval 181-1123C-29X-2, 90–110 cm, and (B) interval 181-1124C-43X-2, 28–48 cm. Location of the Marshall Paraconformity is shown by arrows.

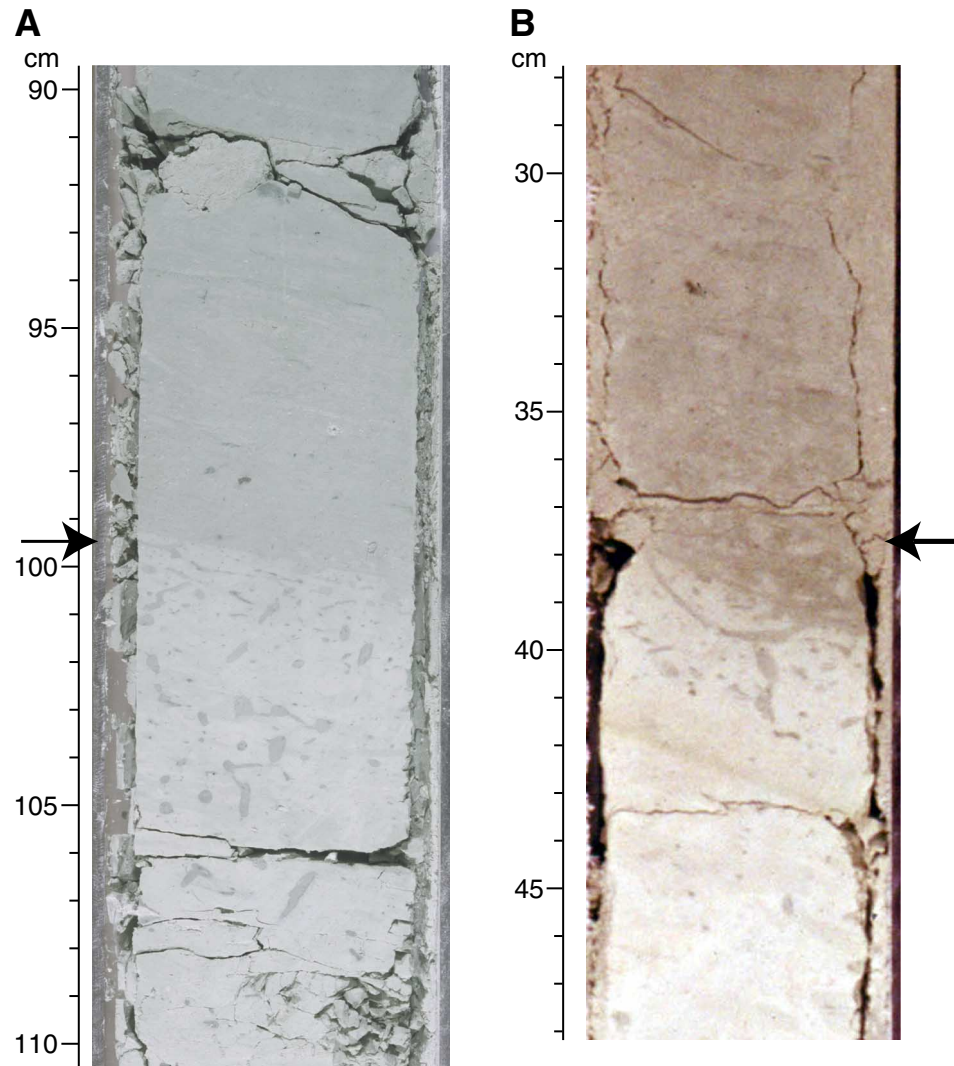


Figure F4. Age-depth plot for Hole 1123C based on calcareous nannofossil datums (triangles) and magnetostratigraphic datums (squares). Dashed lines represent age uncertainty in datums. Plotted depths are mcd averages. See Table T3, p. 20, for data points.

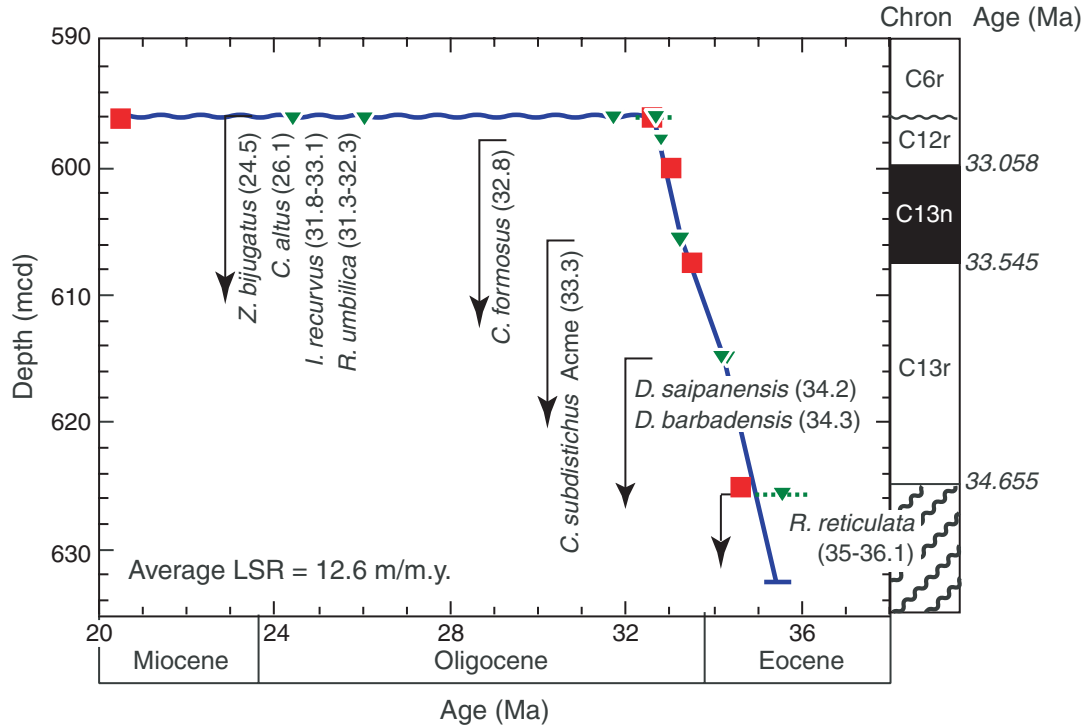


Figure F5. Age-depth plot for Hole 1124C based on calcareous nannofossil datums (triangles) and magnetostratigraphic datums (squares). Plotted depths are mbsf averages. See Table T4, p. 21 for data points. Upward-pointing triangle = FO, downward-pointing triangle = LO.

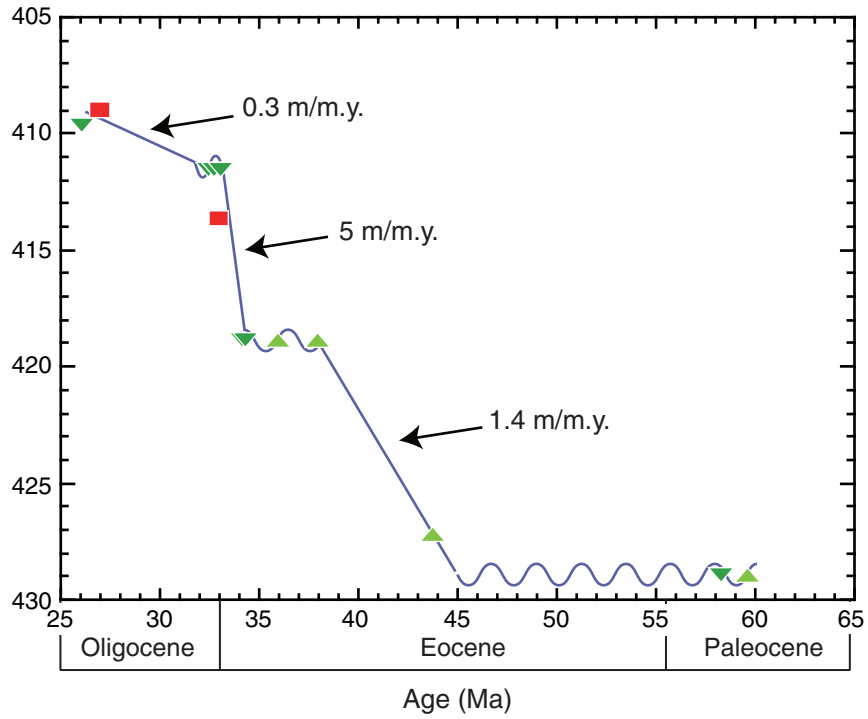


Table T2 (continued).

Age	Nannofossil zone		Core, section, interval (cm)	Depth (mbsf)	Abundance	Preservation	<i>Bicolummus ovatus</i>	<i>Blackites spinosus</i>	<i>Chiasmolithus altus</i>	<i>Chiasmolithus grandis</i>	<i>Chiasmolithus</i> sp.	<i>Clausiococcus subadistica</i>	<i>Coccolithus eopelagicus</i>	<i>Coccolithus formosus</i>	<i>Coccolithus pelagicus</i>	<i>Coronocyclus</i> sp.	<i>Cyclicargolithus abisectus</i>	<i>Cyclicargolithus floridanus</i>	<i>Cyclicargolithus lumina</i>	<i>Discoaster barbadiensis</i>	<i>Discoaster deflandrei</i>	<i>Discoaster saipanensis</i>	<i>Discoaster</i> sp. (6 ray)	<i>Discoaster tani nodifer</i>	<i>Discoaster tani</i>	<i>Fasicolithus tymaniformis</i>	<i>Helicosphaera</i> sp.	<i>Hornibrookina teurensis</i>	<i>Isthmolithus recurvus</i>	<i>Markalius inversus</i>	<i>Nannotetrina fulgens</i>	<i>Reticulolenestra clatrata</i>	<i>Reticulolenestra bisecta</i>	<i>Reticulolenestra daviesi</i>	<i>Reticulolenestra perplexa</i>	<i>Reticulolenestra samodurovii</i>	<i>Reticulolenestra</i> sp.	<i>Reticulolenestra</i> sp. (<4 µm)	<i>Reticulolenestra umbilica</i> (>14 µm)	<i>Rhabdosphaera tenuis</i>	<i>Sphenolithus moriformis</i>	<i>Sphenolithus radians</i>	<i>Zygrabolithus bijugatus</i>					
	Martini (1971)	Okada and Bukry (1980)																																														
middle Eocene	NP16	CP14a	44X-6, 10–11	426.90	A	P				F	F		F	F																																		
			44X-6, 60–61	427.40	C	P																																										
			44X-6, 110–111	427.90	F	P																																										
			44X-7, 10–11	428.40	B	B																																										
			44X-CC, 13–	428.88	R	P																																										
middle Paleocene			45X-1, 10–11	429.09	A	M																																										

Notes: Abundance: V = very abundant, A = abundant, C = common, F = few, R = rare, B = barren. Lowercase letters indicate reworked specimens. Preservation: G = good, M = moderate, P = poor, B = barren.

Table T3. Calcareous nannofossil and magnetostratigraphic events with ages, occurrence intervals, and average depths used to construct LSR for Hole 1123C. Ages, occurrence intervals, and average depths (mcd) are listed.

Age (Ma)	Calcareous nannofossil event	Top interval (cm)	Bottom interval (cm)	Depth (mcd)
24.5	LO <i>Z. bijugatus</i>	29X2, 97–98*	29X-2, 110–111	596.44
26.1	LO <i>C. altus</i>	29X2, 97–98*	29X-2, 110–111	596.44
31.8–33.1	LO <i>I. recurvus</i>	29X2, 97–98*	29X-2, 110–111	596.44
32.3	LO <i>R. umbilica</i>	29X2, 97–98*	29X-2, 110–111	596.44
32.8	LO <i>C. formosus</i>	29X4, 61–62	29X-4, 110–111	597.75
33.3	Acme <i>C. subdistichus</i>	30X2, 66–67	30X-2, 114–115	605.95
34.2	LO <i>D. saipanensis</i>	31X2, 10–11	31X-2, 60–61	614.95
34.3	LO <i>D. barbadensis</i>	31X2, 10–11	31X-2, 60–61	614.95
35–36.1	LO <i>R. reticulata</i>	32X2, 111–112	32X-3, 10–11	625.65
Age (Ma)	Magnetostratigraphic event	Core, section, interval (cm)	Error (cm)	Depth (mcd)
20.5–32.6	Hiatus	1123C-29X-2, 91	0	596.33
33.058	C12r	1123C-29X-5, 20	0.05	600.12
33.545	C13n	1123C-30X-3, 100	0.05	607.52
34.655	?C13r	1123C-32X-2, 71	0.05	625.03

Notes: Ages are from Berggren et al., 1995. Magnetostratigraphic data are from G. Wilson (pers. comm, 2001). LO = last occurrence. * = data taken from Shipboard Scientific Party (1999b).

Table T4. Calcareous nannofossil and magnetostratigraphic events used to construct LSR for Hole 1124C. Ages, occurrence intervals, and average depths (mbsf) are listed.

Age (Ma)	Calcareous nannofossil event	Top interval (cm)	Bottom interval (cm)	Depth (mbsf)
26.1	LO <i>C. altus</i>	42X-CC, 10–11	43X-1, 10–11	409.7
31.8–33.1	LO <i>I. recurvus</i>	43X-2, 10–11	43X-2, 60–61	411.6
32.3	LO <i>R. umbilica</i>	43X-2, 10–11	43X-2, 60–61	411.6
32.8	LO <i>C. formosus</i>	43X-2, 10–11	43X-2, 60–63	411.6
34.2	LO <i>D. saipanensis</i>	43X-6, 110–111	44X-1, 10–11	418.9
34.3	LO <i>D. barbadensis</i>	43X-6, 110–111	44X-1, 10–11	418.9
36	FO <i>I. recurvus</i>	43X-6, 110–111	44X-1, 10–11	418.9
38	FO <i>R. bisecta</i>	43X-6, 110–111	44X-1, 10–11	418.9
43.7	FO <i>R. umbilica</i>	44X-6, 10–11	44X-6, 60–61	427.2
58.3	LO <i>H. teurensis</i>	44X-CC, 13–14	45X-1, 29–30*	429.0
59.7	FO <i>F. tympaniformis</i>	44X-CC, 13–14	45X-1, 29–30*	429.0

Age (Ma)	Chron/event (base)	Depth (mbsf)
27.027	C9n	408.9*
33.058	C12r	413.55*

Notes: Ages are from Berggren et al., 1995. LO = last occurrence, FO = first occurrence. * = data taken from Scientific Shipboard Party (1999c).

Plate P1. Illustrations are light micrographs (LM). XP = cross-polarized light, Ph = phase-contrast light, Pl = parallel light. Scale bars = 2 μm . 1. *Reticulofenestra bisecta* (Sample 181-1124C-43X-4, 110–111 cm); XP 2100 \times . 2, 3. *Coccolithus formosus* (Sample 181-11123C-32X-4, 10–11 cm); (2) Ph 4800 \times and (3) XP. 4. *Sphenolithus moriformis* (Sample 181-1124C-43X-4, 110–111 cm); XP 6200 \times . 5, 6. *Reticulofenestra samidurovii* and *R. umbilica* (Sample 181-1123C-32X-2, 111–112 cm); (5) XP 1700 \times and (6) Ph. 7, 8. *Reticulofenestra daviesii* and *R. dictoyoda* (Sample 181-1123C-32X-1, 10–11 cm); (7) XP 1900 \times and (8) Ph. 9–11. *Chiasmolithus oasaruensis* (Sample 181-1123C-32X-2, 111–112 cm); (9) Ph 2000 \times , (10) Ph, and (11) XP. 12. *Discoaster saipanensis* (Sample 181-1123C-32X-1, 10–11 cm); Ph 1800 \times . 13. *Discoaster barbadensis* (Sample 181-1124C-44X-6, 10–11 cm), Ph 1500 \times . 14. *Ismolithus recurvus* (Sample 181-1123C-32X-1, 10–11 cm); Ph 3000 \times . 15. *Ismolithus recurvus* (Sample 181-1123C-30X-3, 58–59 cm); XP 4000 \times . 16, 17. *Xlausicoccus subdistichus* (Sample 181-1123X-32X-1, 10–11 cm); (16) Ph 4600 \times and (17) XP.

